Medical Engineering and Physics 68 (2019) 17–24

Contents lists available at ScienceDirect

Medical Engineering and Physics

journal homepage: www.elsevier.com/locate/medengphy

Patellar bone strain after total knee arthroplasty is correlated with bone mineral density and body mass index

Adeliya Latypova[a], Elham Taghizadeh[b], Fabio Becce[c], Philippe Büchler[b], Brigitte M Jolles[d], Dominique P Pioletti[a], Alexandre Terrier[a,*]

[a] Laboratory of Biomechanical Orthopedics, Ecole Polytechnique Fédérale de Lausanne, Station 9, 1015 Lausanne, Switzerland
[b] ARTORG Center for Biomedical Engineering Research, University of Bern, Bern, Switzerland
[c] Department of Diagnostic and Interventional Radiology, Lausanne University Hospital and University of Lausanne, Lausanne, Switzerland
[d] Service of Orthopedics and Traumatology, Lausanne University Hospital and University of Lausanne, Lausanne, Switzerland

ARTICLE INFO

Article history:
Received 23 August 2018
Revised 15 March 2019
Accepted 31 March 2019

Keywords:
Arthroplasty
Knee
Patella
Patient-specific
Finite elements

ABSTRACT

Patella-related complications after total knee arthroplasty (TKA) remain a major clinical concern. Previous studies have suggested that increased postoperative patellar bone strain could be related to such complications, but there is limited knowledge on patellar strain after TKA. The objective of this study was to predict patellar bone strain after TKA and evaluate correlations with various preoperative data. Fourteen TKA patients with a minimum follow-up of one year were included in this study. Using preoperative CT datasets, preoperative planning, and postoperative X-rays, a method is presented to generate patient-specific finite element models after virtual TKA. Patellar kinematics and forces were predicted during a squat movement, and patellar bone strain was evaluated at 60° of knee flexion. Strain varied greatly among patients, but was strongly negatively correlated ($r = -0.85$, $p < 0.001$) with bone mineral density (BMD) and moderately positively ($r = 0.54$, $p = 0.05$) with body mass index (BMI). The BMI/BMD ratio explained 87% of strain, and should be further investigated as a potential risk factor for clinical complications. This study represents a preliminary step towards the identification of patients at risk of patellar complications after TKA.

© 2019 IPEM. Published by Elsevier Ltd. All rights reserved.

1. Introduction

Total knee arthroplasty (TKA) is a well-accepted treatment option in severe cases of osteoarthritis. Despite substantial improvements in surgical techniques and implant designs during the last decades, patients still face relatively frequent postoperative complications. While patellar fractures after resurfacing are considered as rare (0.5–5.2%), one of the most severe complications, anterior knee pain (AKP) is much more common (0–47%) and still poorly understood [1–4].

Previous studies have shown that TKA leads to increased strain in the patella, and thus hypothesized that this strain increase could be associated with postoperative complications [5–10]. Indeed, increased strain can lead to tissue damage and thus to fatigue fracture [7]. Higher strains can also induce an increase in metabolic activity of bone cells, which can in turn be associated with pain [11]. Even though the exact origin of AKP is unknown, patellar bone is considered as one of the most probable cause [11,12] and should therefore be studied in greater detail.

A recent numerical case-control study conducted on young females with patellofemoral pain (without TKA) supported the hypothesis of elevated strain as a cause of knee pain, by predicting higher peak and average patellar bone strain in the pathological group [13]. Another patient-specific model of TKA reported higher patellar strain when the patella was thinner [14].

In the preoperative planning of TKA, patellar resurfacing is generally overlooked, as surgeons lack instruments to estimate surgical outcome and the surgically-induced increase in patellar bone strain. On the other hand, knowledge of strain levels experienced within the patella, particularly during daily living activities after TKA, is also scarce. Previous in vitro studies were limited by measuring strain only at bone surfaces and by the magnitudes of applied boundary forces [7]. Moreover, cadaveric donors do not necessarily accurately represent a cohort of TKA patients and lack consistent clinical information. Existing numerical studies investigating patellar bone strain in TKA were either based on cadavers, and/or not adapted to important patient characteristics, such as body weight [6,15,16], which can reasonably be assumed to affect bone strain. Furthermore, in these studies, the patella

* Corresponding author.
E-mail address: alexandre.terrier@epfl.ch (A. Terrier).

https://doi.org/10.1016/j.medengphy.2019.03.017
1350-4533/© 2019 IPEM. Published by Elsevier Ltd. All rights reserved.

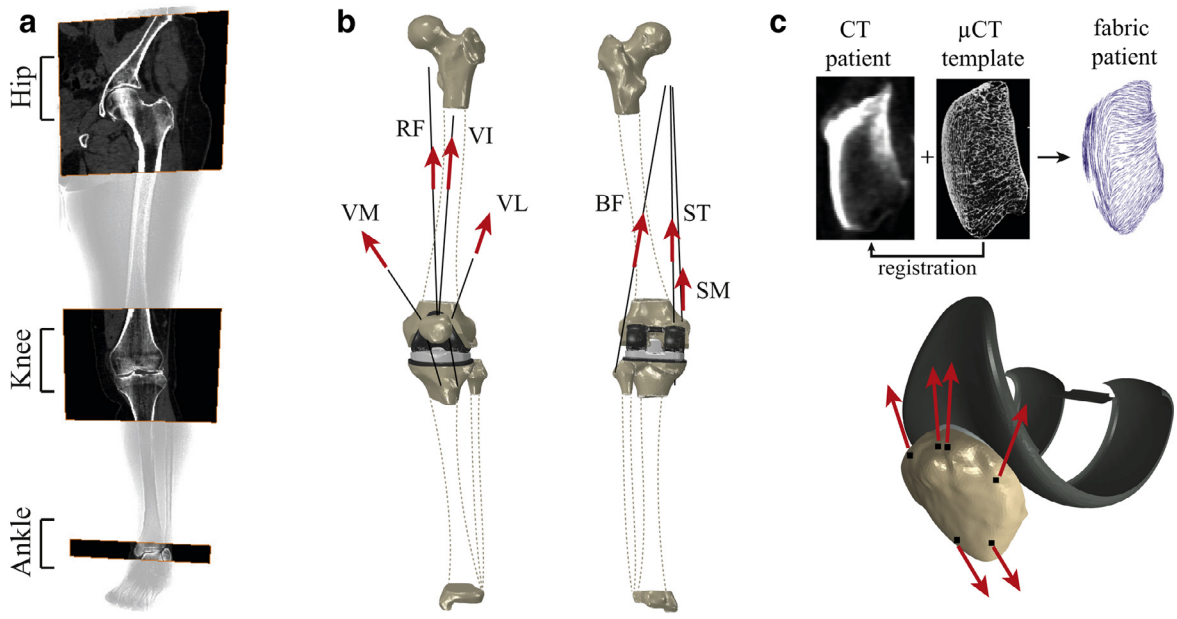

Fig. 1. (a) Preoperative standardized TKA CT protocol with images acquired on the hip, knee, and ankle joints, as well as on thigh muscles (not shown); (b) patient-specific finite element TKA model; and (c) patella model (bottom) with material mapping of the patellar bone based on patient CT and template µCT images (top).

was modeled using isotropic material properties, which has been shown to affect the accuracy of strain predictions [17]. Estimation of strain levels that TKA patients experience during daily living activities could help evaluate a strain limit that should be targeted to prevent postoperative complications. Such knowledge in combination with a patient-specific numerical model could help improving surgical planning, technique, and clinical outcome.

Therefore, our objective was to predict patellar bone strain after TKA and evaluate correlations of the predicted strain with various preoperative data. We thus developed patient-specific finite element models of patients who underwent TKA, and had a minimum follow-up of 12 months. The models were based on patient preoperative data, and replicated a squat movement. For each patient, models predicted postoperative patellar kinematics, patellar forces, and patellar strain levels. These predictions were then correlated with various preoperative patient characteristics, such as gender, age, body mass index (BMI), as well as the volume and bone mineral density (BMD) of the resurfaced patellar bone. This study represents a preliminary step towards the evaluation of potential risk factors for patellar complications after TKA.

2. Methods

2.1. Overview

Patient-specific finite element models were developed from preoperative data of patients who underwent TKA. For each patient, two coupled models were developed: a knee model, and a patella model (Fig. 1(a)). These two models were implemented in Abaqus/Standard (Simulia, Providence, RI, USA), and previously validated by comparing kinematics and forces predictions to a robotic simulator, and patellar strain predictions to a micro-finite element model [14,17,18].

2.2. Patients

For this single-center retrospective study, patients were selected from our University Hospital database between January 2014 and April 2015. Inclusion criteria were: TKA with cemented ultra-congruent posterior-stabilized mobile-bearing knee prosthesis (F.I.R.S.T.; Symbios, Yverdon-les-Bains, Switzerland), patellar resurfacing with a three-peg modified dome patellar component, preoperative planning with patient-specific cutting guides, availability of standardized preoperative computed tomography (CT), availability of postoperative X-rays (frontal, lateral, and skyline views), and a minimum of 12 months postoperative clinical follow-up. We excluded cases with postoperative complications not related to patellar bone. According to these criteria, we selected 14 patients (Table 1). Since none of these had AKP or a patellar fracture during the follow-up period, our study included only patients without any postoperative complications. All patients underwent the same standardized preoperative CT protocol for scanning their lower limbs (Supplementary Material). This study was approved by the institutional ethics committee (CER-VD, protocol 90/11).

2.3. Knee model

The knee model included the femur, tibia, patella, and 7 muscles: rectus femoris (RF), vastus intermedius (VI), vastus lateralis (VL), vastus medialis (VM), biceps femoris (BF), semitendinosus (ST), and semimembranosus (SM) (Fig. 1(b)). The model also included all prosthetic components: metallic femoral component, metallic tibial tray, polyethylene tibial insert, and polyethylene patellar component. Bone geometries were reconstructed by segmentation of preoperative CT images (Amira; FEI Visualization Sciences Group, Burlington, MA, USA). Position and bone cut for femoral and tibial components replicated preoperative planning software [19]. Since patella resurfacing was not part of preoperative planning, position and bone cut for patellar component were estimated from postoperative X-rays (frontal and skyline views). The femur and tibia bones, as well as metallic components were modelled as rigid bodies. Metallic implants were thus kinematically constrained to their host bone. Polyethylene tibial and patellar components were considered to be linear elastic [15]. Patellar tendon was modeled by two non-linear springs with a reference length estimated from preoperative CT images [20]. Quadriceps tendons were linear fibers [21]. We simulated a squat movement (Oxford Rig) with hip and ankle centers aligned with body weight applied along vertical axis [22]. Initial positions of

Table 1
Patient characteristics and strain predictions. "F" stands for female and "M" for male. "BMI" is the body mass index, "V" is the postoperative volume of the resurfaced patella, and "BMD" is the average bone mineral density of the resurfaced patella, "S_{p1}"and "S_{p2}" is the calculated strain thresholds.

Patient	Gender	Age (years)	Height (cm)	BMI (kg/m^2)	V (cm^3)	BMD (g/cm^3)	S_{p1} (%)	S_{p2} (%)
#1	F	62	161	40.5	13.5	0.28	1.88	1.67
#2	F	72	153	28.6	8.7	0.40	0.83	0.71
#3	F	64	165	25.0	10.5	0.22	1.59	1.43
#4	F	84	162	32.8	12.4	0.23	2.42	2.26
#5	M	60	170	27.0	11.4	0.36	1.60	1.38
#6	M	69	173	37.4	18.9	0.34	1.15	1.07
#7	M	65	174	29.7	20.1	0.56	0.57	0.54
#8	M	62	174	31.0	15.5	0.45	0.79	0.62
#9	M	68	183	27.8	12.6	0.45	1.23	0.95
#10	F	74	178	38.5	17.6	0.21	3.51	3.17
#11	F	87	153	28.2	6.1	0.26	2.25	1.51
#12	F	77	159	39.2	10.0	0.26	2.29	2.17
#13	F	70	170	30.4	10.6	0.23	2.44	2.02
#14	F	66	159	26.5	11.1	0.36	0.90	0.78

Table 2
Muscle ratios. "PCSA" stands for physiological cross-sectional area.

Muscle	PCSA ratios	EMG ratios	Final ratios
RF	0.85	1	0.85
VI	1	1	1.00
VL	1.74	1.21	2.11
VM	1.13	1.26	1.43
BF ($S+L$)	0.86	0.18	0.16
ST	0.52	0.16	0.08
SM	0.78	0.16	0.12

femur and patella coincided with preoperative CT images, while tibia was aligned according to position of virtually implanted prosthetic components. Squat was controlled by VI muscle elongation. Muscle forces were synchronized by a user-defined element to guarantee predefined force ratios [23]. Muscle force ratios were defined as the product of their physiological cross-sectional area and electromyography (EMG) [24–27]. Since EMGs of these muscles are nearly proportional during squat, their force ratios were assumed constant. EMG of VI and RF was assumed equal (Table 2). Patellofemoral and tibiofemoral contact, as well as contact between quadriceps tendons and femoral component were assumed frictionless. The inferior face of the tibial polyethylene component was kinematically constrained to the tibial rigid metallic component.

Patellar kinematics predicted by the knee model was described in the patellofemoral joint coordinate system [28]. Femoral and patellar frames, as well as their origins were defined by implant geometries and bone anatomical features (Fig. 2). We estimated patellar medial–lateral (M–L), superior–inferior (S–I), and anterior–posterior (A–P) translations, as well as flexion–extension rotation, internal–external spin, and medial–lateral tilt. We also analyzed forces of quadriceps (F_q), patellar tendon (F_p), and patellofemoral contact forces (F_c). All forces were normalized by patient body weight (obtained by multiplying patient body mass by gravity constant).

2.4. Patella model

The patella model included the patellar bone, polyethylene component, cement layer, and femoral component (Fig. 1(c)). Polyethylene had the same properties as in the knee model. We considered a uniform cement layer with a thickness of 0.5 mm around patellar component. Cement was linear elastic [15]. Bone was modeled as linear elastic material based on morphology-

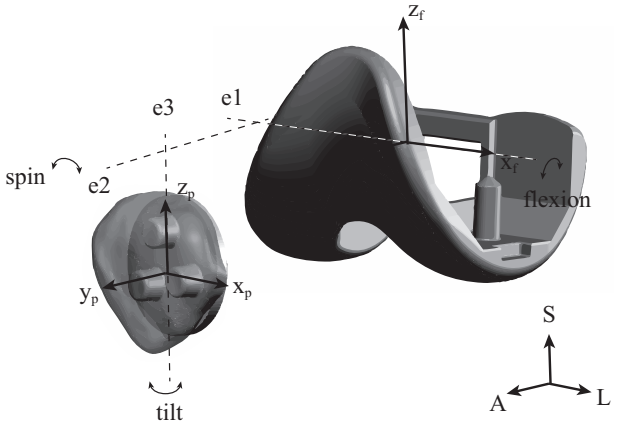

Fig. 2. Coordinate system (e1, e2, e3) for the patellofemoral joint. Femoral frame: x_f is the horizontal lateral axis of the femoral component (defined by the manufacturer as axis of flexion and extension of the knee between 0 and 90°), z_f is the line between the implant center and center of hip joint, y_f is the cross product of x_f and z_f. Patellar frame: y_p is the axis of conical articular doom of the patellar component, z_p is the line on the anterior part of the patellar component crossing y_p and the apex of the patella, x_p is the cross product of y_p and z_p.

Table 3
Parameters for morphology–elasticity relationship.

E_0 (MPa)	ν_0	G_0 (MPa)	k	l
12723.1	0.24	4224.6	2.1	1.02

elasticity relationship [29]:

$$E_i = E_0\rho^k\left(m_i^2\right)^l,\ \frac{E_i}{\nu_{ij}} = \frac{E_0}{\nu_0}\rho^k\left(m_i m_j\right)^l,$$
$$G_{ij} = G_0\rho^k\left(m_i m_j\right)^l,\ \forall i \neq j = 1,2,3, \quad (1)$$

where E_i, ν_{ij}, and G_{ij} are engineering constants, ρ is bone volume fraction, and m_i are normalized eigenvalues of second-order fabric tensor $\mathbf{M}$ [30]. E_0, ν_0, G_0, k, l are model parameters that were identified on 200 cubic samples extracted from 20 fresh-frozen cadaveric patellae (Table 3) [18]. For each patella, preoperative BMD was obtained from CT numbers (Hounsfield units) using a quantitative CT calibration phantom (Mindways Software, Austin, TX, USA), and was then used to calculate bone volume fraction ρ [18]:

$$BMD = \frac{HU}{1320},\ \rho = 1.061\ BMD,\ +0.0669, \quad (2)$$

For each patella, bone anisotropy was estimated with a validated registration method [31]. This method was based on non-rigid registration of micro-CT (μCT) scan of a cadaveric patella to patient CT. Bone volume fraction and anisotropy were evaluated at nodes of a background grid (2 mm edge length and 5.3 mm sphere diameter), and subsequently interpolated within finite elements [32]. Preprocessing of the CT and μCT images were performed in Amira, while registration was conducted in Elastix [33]. Material mapping was done in Medtool (www.dr-pahr.at). Patellofemoral contact was assumed frictionless. All other interfaces where fully bonded. Bone, cement, and polyethylene were meshed with quadratic tetrahedral elements. A mesh convergence analysis was performed to guarantee variations below 1% error. The average element size was 2 mm for the patella, requiring about 20,000 elements. The position of the patella and femoral components corresponded to 60° of knee flexion predicted by the knee model. Patellar forces (quadriceps, patellar tendon) predicted by the knee model were distributed along the anterior patellar surface through auxiliary points representing insertions of the tendon and muscles in the knee model (cubic continuum constraint in Abaqus).

We considered octahedral shear strain invariant to quantify patellar bone deformation [34]. This strain measure has been shown to be a good predictor of trabecular bone micro-damage [35]. We evaluated two strain thresholds for each bone: S_{p1} and S_{p2}. S_{p1} corresponded to the value of the highest strain in 99% of resurfaced patellar bone volume, or in other words, strains in 1% of the bone volume was above S_{p1}[6]. This limit was considered as peak strain in the bone. Similarly, we estimated strain threshold S_{p2}: 2% of bone volume was above this threshold. This threshold was chosen similar to the "Pistoia criterion" to estimate potential bone damage [36].

2.5. Correlations

First, we tested whether strain threshold S_{p2} was significantly correlated with the following patient characteristics: gender, age, BMI, average preoperative BMD and volume (V) of postoperative resurfaced patella, as well as predicted patellar forces at 60° of flexion (F_q, F_p, and F_c). BMD was averaged on resurfaced patellar bone volume. Next, step-wise multiple regressions with interactions were used to assess which combination of patient characteristics explained the most strain variance. Prior to regression, these characteristics were examined on intercorrelation (through correlation coefficient r and p-value) and on multicollinearity (through variance inflation factor VIF). Finally, the best correlation was used to estimate the range of patient characteristics that can lead to higher strains and thus a higher risk of complications. *P*-values less than 0.05 were considered statistically significant, and parameters with VIF less than 4 were considered independent [37]. Statistical analysis was performed with the statistics toolbox of Matlab (The MathWorks, Natick, MA, USA).

3. Results

3.1. Knee model

From full extension to 90° of knee flexion, patellar kinematics followed the same trend among patients (Fig. 3). Patellae flexed from 15.6 ± 4.1 to 60.0 ± 4.7°. In full knee extension, patellae were laterally tilted by 4.6 ± 2.6°, but moved to neutral position (or medially tilted) after 55° of knee flexion. Spin angle remained nearly constant during flexion, but varied from −5 to 15° between patients. Patellae translated posteriorly by 8.7 ± 1.7 mm, inferiorly by 18.8 ± 3.2 mm, and laterally by 2.5 ± 1.4 mm. F_q, F_p, and F_c forces grew almost linearly during flexion and followed also the same trend between patients. F_q, F_p, and F_c forces were in the same range between patients reaching 5.0 ± 0.3, 3.7 ± 0.3, and 6.1 ± 0.3 body weight, respectively, at 90° of knee flexion.

Table 4
Summary of regression analysis.

	Estimate	Std. error	*p*-value
Sp2 ~ BMI + 1/BMD + BMI/BMD			
(Intercept)	5.52514	1.44236	0.003315
1/BMD	−1.44512	0.38562	0.003799
BMI	−0.20502	0.04749	0.001521
BMI/BMD	0.06744	0.01251	0.000305
Adjusted R2 = 0.95			
Sp2 ~ BMI/BMD			
(Intercept)	−0.48361	0.219951	0.0482
BMI/BMD	0.017906	0.001922	7.65E−07
Adjusted R2 = 0.87			

3.2. Patella model

At 60° of knee flexion, S_{p1} was 1.7 ± 0.8% (from 0.57% to 3.51%) (Table 1, Fig. 4). S_{p1} reached a maximum of 3.5% in one patella, was between 2% and 3% for 4 patellae, and was lower than 2% for 9 patellae. S_{p2} was 1.4 ± 0.8% (from 0.54% to 3.17%). S_{p2} reached a maximum of 3.2% in one patella, was between 2% and 3% for 3 patellae, and was lower than 2% for 10 patellae.

3.3. Correlations

Three patient characteristics were significantly correlated with S_{p2}: BMD ($r = -0.85$, $p < 0.001$), BMI ($r = 0.54$, $p = 0.05$), and gender ($r = -0.55$, $p = 0.04$). It was found that reciprocal of BMD had a higher correlation with strain ($r = 0.87$, $p < 0.001$). Therefore, we decided to use reciprocal BMD in further analysis. Volume V did not show significant correlation with S_{p2} ($r = -0.06$, $p = 0.83$). S_{p2} was slightly better correlated with non-normalized patellar forces than with BMI: F_q ($r = 0.56$, $p = 0.04$), F_p ($r = 0.49$, $p = 0.07$), and F_c ($r = 0.59$, $p = 0.02$). Age, BMI, reciprocal BMD, and V were found to be independent and were used in the regression analysis. The step-wise multiple regression with interactions revealed that combining BMI + 1/BMD + BMI/BMD explained 95% of strain variations (Table 4). Parameter BMI/BMD had the lowest *p*-value and explained alone 87% of variations. Using the regression equation for BMI/BMD, we proposed a mapping relating strain levels to BMI and BMD (Fig. 5).

4. Discussion

Patellar fracture and AKP remain major clinical complications after TKA. Increased strain in patellar bone is suggested to be one of the main causes of these complications. However, current knowledge on patellar strain in TKA patients is scarce. In addition, surgeons do not have valid instruments to predict postoperative patellar strain during preoperative planning. In the present study, correlations between patellar bone strain and several preoperative parameters were tested using patient-specific finite element models of TKA patients. The reported strong correlations suggest that a relatively simple and systematic preoperative evaluation of the patellar bone might help improve outcome in TKA.

Inter-patient kinematics variability was high, yet consistent with recent experimental (gait analysis from fluoroscopy) and numerical studies [38–40]. All patients presented a lateral shift of the patella, while higher variations in medial and lateral directions are reported in the literature, especially at low flexion angles. This may be explained by the absence of patellofemoral ligaments and fixed muscle ratios between patients in the knee model. At low flexion angles, patella is guided by muscles and soft tissues,

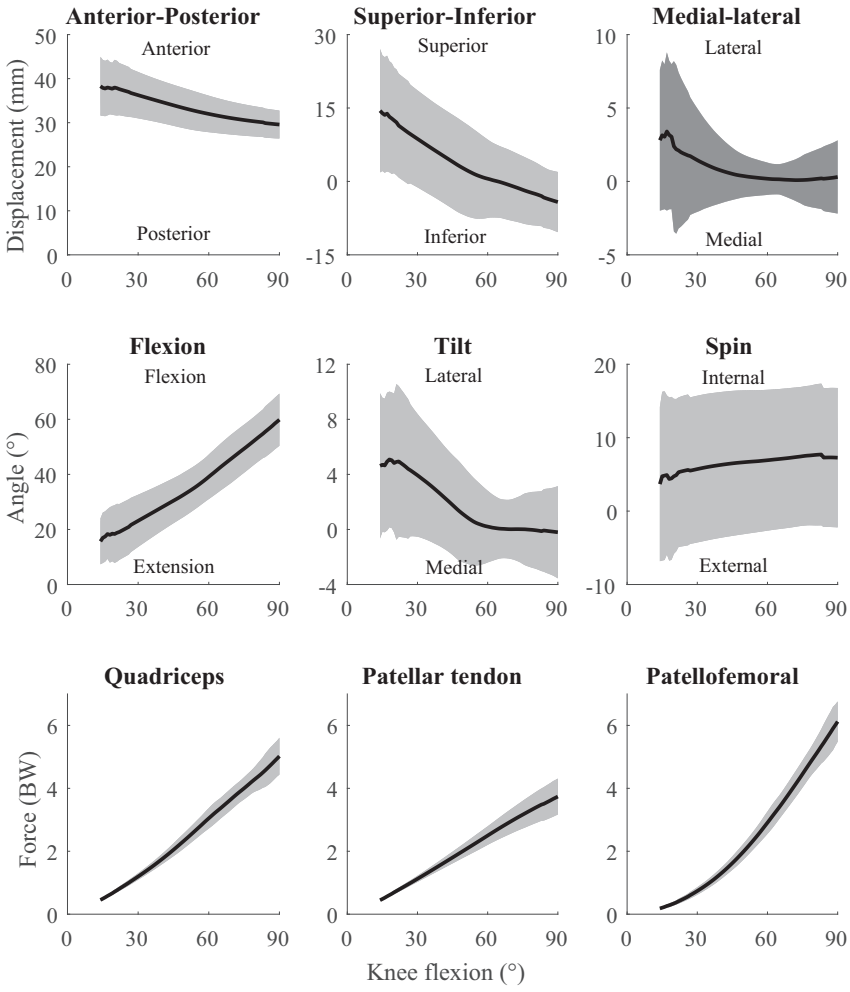

Fig. 3. Predicted patellar kinematics, quadriceps force, patellar tendon force, and patellofemoral force, averaged for all patients (solid black line) with bands of variation (grey area).

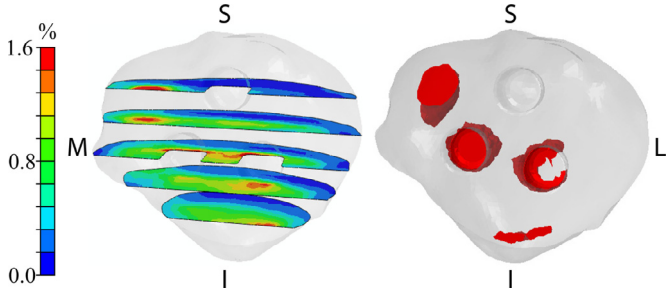

Fig. 4. Example of patellar bone strain distribution with peak strain threshold level SP_1 (left) and 2% of highly strained bone volume (right) in patient #5.

while at higher flexion degrees it is mainly directed by trochlear groove geometry [41]. Higher variation in trends between patients was observed for patellar tilt. Seven patients presented laterally tilted patellae at higher angles of knee flexion in comparison with other seven. Interestingly, all these seven patients had from slight to strong patellar tilt on postoperative X-rays. Comparison with postoperative X-rays conducted in non-weight-bearing positions is difficult. Such X-rays cannot fully reflect weight-bearing patellar kinematics, but can still indicate potential kinematics alterations [42]. Predicted forces were in the reported range for squat (Oxford rig) movement [22]. Variations in normalized forces between patients are probably due to their intrinsic anatomical differences: patient height, patella position, and/or prosthetic components position [43].

Strain predictions were conducted during loaded squat motion at 60° of knee flexion. Squat is one of the main components of movements for activities of daily living, such as walking, stair climbing or getting up from a chair, with 60° of knee flexion often reached during such activities [22,44]. To decrease unknowns in the numerical model, the Oxford rig squat was modeled considering that hip and ankle were aligned during movement and body weight acted vertically. This kind of movement is physiologically possible but mainly up to 60° of knee flexion [45]. In deeper angles, the hip starts to move backwards and the trunk bends helping to decrease muscle forces. Therefore, to keep more typical loadings and knee angles in our study [46,47], we decided to consider 60° of knee flexion. Peak (octahedral shear) strain was between 0.6% and 3.5%, which corresponds to findings from a comparable numerical study [6].

The constitutive law used to predict bone strain is based on clinical CT images calibrated with a phantom, to transform CT numbers expressed in Hounsfield units into BMD, and bone volume fraction. The constitutive law also considers the bone anisotropy, which is provided by a registration method. It is conceptually different from alternative micromechanics-based theories, which have also been proposed to convert CT scan datasets into anisotropic elasticity tensors [48]. The method used in this

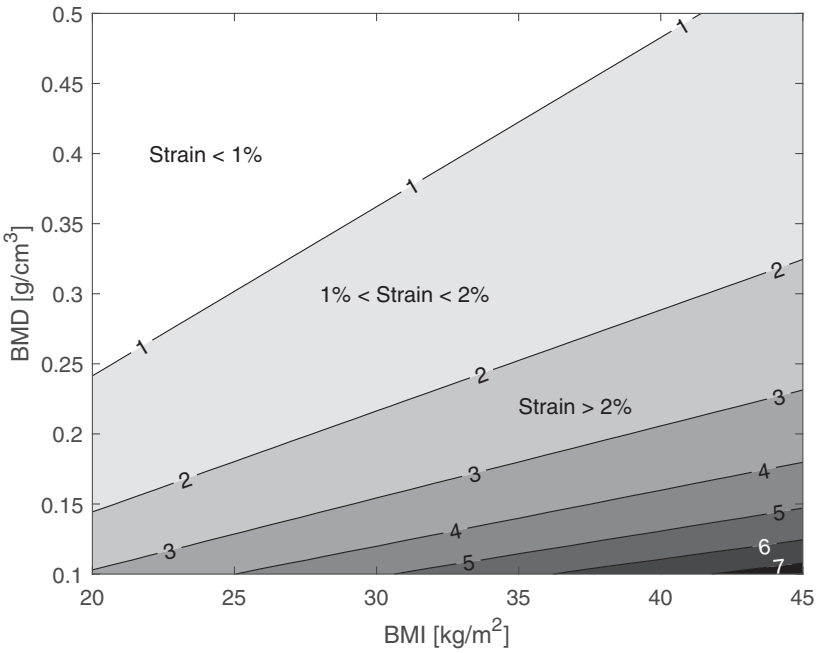

Fig. 5. Strain mapping prediction based on BMD and BMI ranges. The lines and their label correspond to the strain value between strain zones.

study has been previously validated for the patella, but also for other bones [31].

To estimate bone damage, we used the "Pistoia criterion" [36]. This criterion suggests that damage is initiated when 2% of bone volume is strained above its yield limit. Thus, we estimated the strain threshold for 2% highly strained bone volume. We suggested that if this strain threshold is beyond bone yield strain, the patient presents a risk of complications. Strain limit between 1% and 2% can be considered as critical [49–51]. For ten patients, specific (octahedral shear) strain threshold was below 2%, and four patients had bone strain above this threshold, suggesting a higher risk of complications. However, further investigations on highly strained bone volumes and "risk-prone" strain thresholds should be conducted, since the Pistoia study was conducted on the radius bone with different loading conditions.

A significant correlation was found between strain thresholds, BMI, and BMD. The BMI/BMD ratio could predict 87% of the strain variation. This result make sense, since strain increases with higher body weight (thus applying forces), and decreases with increasing bone density. Still, we expected a higher significance of patellar bone volume though, since thinning of the patella leads to an increase in bone strain [5,14]. Considering the percentage of remaining volume relative to the intact bone volume did not improve correlations. We may still assume that other geometrical parameters of the patella (thickness, width, etc.) might be better correlated with strain. Data were also analyzed by means of a stepwise multiple linear regression approach. The analysis confirmed a high significance of BMI, BMD, and their interaction in predicting strain. The combination of BMI and BMD was used to predict a strain mapping, and estimate values that can cause excessive strains, and thus potential clinical complications. This mapping (Fig. 5) would indicate a risk-free zone (strains $< 1\%$) and more risk-prone zones (strains $> 2\%$). This potential risk factor for patellar complication after TKA should be tested on a larger cohort of patients.

Average BMD and BMI of patients included in this study were in the transition zone (between 1% and 2%), and none of these patients presented patella-related clinical complications. Note that this risk may change during rehabilitation: a gradual increase in the level of daily activities after TKA might increase BMD (bone remodeling), more than strain, and thus enable patient transition to the risk-free zone [52].

There are several important limitations of the study. Simulated squat movement is relatively simple. More typical movements might extend the patellar strain variation between patients. Predefined muscle ratios were fixed during squat movement, and between patients. Our previous study showed that a change of force ratios will rather influence volumes of strained bone on lateral and medial aspects of the patella than total strained volume [14]. However, this sensitivity analysis was conducted with only one patient, and should be repeated on more subjects, since bone density may also vary. Other limitations of the model include the simplified geometry considered for the cement layer and the implant positioning replicated from the preoperative planning, which may not be exactly what has been performed during surgery. However, all patients were operated with patient-specific instrumentations (cutting guides), which were reported to replicate the preoperative planning with 3° in the frontal plane in 93% of the cases [19]. Moreover, penetration of cement into bone might influence bone material properties close to the interface. Patients were followed-up only 12 months postoperatively. Since there was no complication during this period, we could not associate a specific critical value of patellar strain or preoperative patient characteristics to a risk of adverse clinical outcome. A longer follow-up of these patients might allow to later associate parameters with patellar complications. Development of complications may take from a few months to several years [53,54]. We considered simple combination of parameters to predict strain outcome on range of BMI and BMD. However, further prediction of strain map through linear combination was not adequate at high BMD values, meaning that initially there was no sufficient number of subjects and no full coverage of BMI and BMD ranges at linear regression analysis. However, it is worth mentioning that the range of BMI and BMD leading to high strains were similar in any prediction model that we investigated. Last but not least, male and female patients should be investigated separately. In our study, females experienced higher strains than males. Males had higher body weights and experienced higher non-normalized patellar forces, but had statistically significantly higher patellar

bone volumes and densities. However, division into groups was not possible in the study because of the small number of subjects.

To conclude, our study revealed the impact of BMI on patellar bone strain, and also the influence of BMD of the remaining patella (after TKA resurfacing) on patellar bone strain. This study represents a preliminary step towards the identification of potential risk factors for patellar complications after TKA. As a next step, we should test the association of the BMI/BMD ratio with clinical complications in a larger patient cohort. If the proposed risk factor is confirmed, we would recommend to introduce a routine preoperative examination of patellar density before TKA. Within a preoperative software, the patellar cut could be planned in such a way to avoid the high strain zone (Fig. 5). This surgical planning assistance tool should be associated with a patient-specific cutting guide.

Acknowledgments

We thank Vincent Leclercq and Symbios Orthopédie SA (Yverdon-les-Bains, Switzerland) for providing the files of implant geometries and patient-specific preoperative planning. This project was supported by “Lausanne Orthopedic Research Foundation”.

Conflict of interest

None of the authors has any conflict of interest.

Author contribution

Latypova: research design, data acquisition, analysis and interpretation, manuscript writing.

Taghizadeh: data acquisition, manuscript revision.

Becce: research design, data acquisition, manuscript revision.

Büchler: study supervision, manuscript revision.

Jolles: study supervision, manuscript revision.

Pioletti: study supervision, manuscript revision.

Terrier: study proposal, design, and supervision, data analysis and interpretation, manuscript writing and revision.

Funding

This project was supported by “Lausanne Orthopedic Research Foundation”.

Supplementary materials

Supplementary material associated with this article can be found, in the online version, at doi:10.1016/j.medengphy.2019.03.017.

References

[1] Schindler OS. The controversy of patellar resurfacing in total knee arthroplasty: IBISNE in medio tutissimus? Knee Surg Sports Traumatol Arthrosc 2012;20(7):1227–44.
[2] Keating EM, Haas G, Meding JB. Patella fracture after post total knee replacements. Clin Orthop Relat Res 2003(416):93–7. doi:10.1097/01.blo.0000092992.90435.20.
[3] Chun KA, Ohashi K, Bennett DL, El-Khoury GY. Patellar fractures after total knee replacement. AJR Am J Roentgenol 2005;185(3):655–60.
[4] van Jonbergen HP, Reuver JM, Mutsaerts EL, Poolman RW. Determinants of anterior knee pain following total knee replacement: a systematic review. Knee Surg Sports Traumatol Arthrosc 2014;22(3):478–99.
[5] Burnett W, Kontulainen S, McLennan C, et al. Patella bone density is lower in knee osteoarthritis patients experiencing moderate-to-severe pain at rest. J Musculoskelet Neuronal Interact 2016;16(1):33–9.
[6] Fitzpatrick CK, Kim RH, Ali AA, Smoger LM, Rullkoetter PJ. Effects of resection thickness on mechanics of resurfaced patellae. J Biomech 2013;46(9):1568–75.
[7] Lie DT, Gloria N, Amis AA, Lee BP, Yeo SJ, Chou SM. Patellar resection during total knee arthroplasty: effect on bone strain and fracture risk. Knee Surg Sports Traumatol Arthrosc 2005;13(3):203–8.
[8] Amirouche F, Choi KW, Goldstein WM, Gonzalez MH, Broviak S. Finite element analysis of resurfacing depth and obliquity on patella stress and stability in TKA. J Arthroplasty 2013;28(6):978–84.
[9] Wulff W, Incavo SJ. The effect of patella preparation for total knee arthroplasty on patellar strain: a comparison of resurfacing versus inset implants. J Arthroplasty 2000;15(6):778–82.
[10] Goldstein SA, Coale E, Weiss AP, Grossnickle M, Meller B, Matthews LS. Patellar surface strain. J Orthop Res 1986;4(3):372–7.
[11] Draper CE, Fredericson M, Gold GE, et al. Patients with patellofemoral pain exhibit elevated bone metabolic activity at the patellofemoral joint. J Orthop Res 2012;30(2):209–13.
[12] Gerbino PG 2nd, Griffin ED, d'Hemecourt PA, et al. Patellofemoral pain syndrome: evaluation of location and intensity of pain. Clin J Pain 2006;22(2):154–9.
[13] Ho KY, Keyak JH, Powers CM. Comparison of patella bone strain between females with and without patellofemoral pain: a finite element analysis study. J Biomech 2014;47(1):230–6.
[14] Latypova A, Arami A, Becce F, et al. A patient-specific model of total knee arthroplasty to estimate patellar strain: a case study. Clin Biomech (Bristol, Avon) 2016;32:212–19.
[15] Fitzpatrick CK, Baldwin MA, Ali AA, Laz PJ, Rullkoetter PJ. Comparison of patellar bone strain in the natural and implanted knee during simulated deep flexion. J Orthop Res 2011;29(2):232–9.
[16] Takahashi A, Sano H, Ohnuma M, et al. Patellar morphology and femoral component geometry influence patellofemoral contact stress in total knee arthroplasty without patellar resurfacing. Knee Surg Sports Traumatol Arthrosc 2012;20(9):1787–95.
[17] Latypova A, Pioletti DP, Terrier A. Importance of trabecular anisotropy in finite element predictions of patellar strain after total knee arthroplasty. Med Eng Phys 2017;39:102–5.
[18] Latypova A, Maquer G, Elankumaran K, et al. Identification of elastic properties of human patellae using micro-finite element analysis. J Biomech 2016;49(13):3111–15.
[19] Franceschi JP, Sbihi AF. Computer Assisted Orthopedic Surgery. 3D templating and patient-specific cutting guides (knee-plan) in total knee arthroplasty: postoperative CT-based assessment of implant positioning. Orthop Traumatol Surg Res 2014;100(6 Suppl):S281–6.
[20] Staubli HU, Schatzmann L, Brunner P, Rincon L, Nolte LP. Quadriceps tendon and patellar ligament: cryosectional anatomy and structural properties in young adults. Knee Surg Sports Traumatol Arthrosc 1996;4(2):100–10.
[21] Voigt M, Bojsen-Moller F, Simonsen EB, Dyhre-Poulsen P. The influence of tendon Youngs modulus, dimensions and instantaneous moment arms on the efficiency of human movement. J Biomech 1995;28(3):281–91.
[22] Mason JJ, Leszko F, Johnson T, Komistek RD. Patellofemoral joint forces. J Biomech 2008;41(11):2337–48.
[23] Terrier A, Reist A, Vogel A, Farron A. Effect of supraspinatus deficiency on humerus translation and glenohumeral contact force during abduction. Clin Biomech (Bristol, Avon) 2007;22(6):645–51.
[24] Cutts A, Seedhom BB. Validity of cadaveric data for muscle physiological cross–sectional area ratios: a comparative study of cadaveric and in-vivo data in human thigh muscles. Clin Biomech (Bristol, Avon) 1993;8(3):156–62.
[25] Yavuz HU, Erdag D, Amca AM, Aritan S. Kinematic and EMG activities during front and back squat variations in maximum loads. J Sports Sci 2015;33(10):1058–66.
[26] Dionisio VC, Almeida GL, Duarte M, Hirata RP. Kinematic, kinetic and EMG patterns during downward squatting. J Electromyogr Kinesiol 2008;18(1):134–43.
[27] Isear JA Jr, Erickson JC, Worrell TW. EMG analysis of lower extremity muscle recruitment patterns during an unloaded squat. Med Sci Sports Exerc 1997;29(4):532–9.
[28] Grood ES, Suntay WJ. A joint coordinate system for the clinical description of three-dimensional motions: application to the knee. J Biomech Eng 1983;105(2):136–44.
[29] Zysset PK. A review of morphology-elasticity relationships in human trabecular bone: theories and experiments. J Biomech 2003;36(10):1469–85.
[30] Cowin SC. The relationship between the elasticity tensor and the fabric tensor. Mech Mater 1985;4(2):137–47.
[31] Taghizadeh E, Reyes M, Zysset P, Latypova A, Terrier A, Buchler P. Biomechanical role of bone anisotropy estimated on clinical CT scans by image registration. Ann Biomed Eng 2016;44(8):2505–17.
[32] Pahr DH, Zysset PK. A comparison of enhanced continuum FE with micro FE models of human vertebral bodies. J Biomech 2009;42(4):455–62.
[33] Klein S, Staring M, Murphy K, Viergever MA, Pluim JPW. elastix: a toolbox for intensity-based medical image registration. IEEE Trans Med Imaging 2010;29(1):196–205.
[34] Kettenberger U, Latypova A, Terrier A, Pioletti DP. Time course of bone screw fixation following a local delivery of Zoledronate in a rat femoral model - a micro-finite element analysis. J Mech Behav Biomed Mater 2015;45:22–31.
[35] Nagaraja S, Couse TL, Guldberg RE. Trabecular bone microdamage and microstructural stresses under uniaxial compression. J Biomech 2005;38(4):707–16.
[36] Pistoia W, van Rietbergen B, Lochmuller EM, Lill CA, Eckstein F, Ruegsegger P. Estimation of distal radius failure load with micro-finite element analysis models based on three-dimensional peripheral quantitative computed tomography images. Bone 2002;30(6):842–8.

[37] Peat J, Barton L. Continuous data analyses: correlation and regression. Medical statistics: A guide to data analysis and critical appraisal. MaldenMA, USA: Blackwell Publishing Inc; 2005. p. 156–201.
[38] Sharma GB, Saevarsson SK, Amiri S, et al. Radiological method for measuring patellofemoral tracking and tibiofemoral kinematics before and after total knee replacement. Bone Joint Res 2012;1(10):263–71.
[39] Ishimaru M, Shiraishi Y, Ikebe S, et al. Three-dimensional motion analysis of the patellar component in total knee arthroplasty by the image matching method using image correlations. J Orthop Res 2014;32(5):619–26.
[40] Fitzpatrick CK, Steensen RN, Tumuluri A, Trinh T, Bentley J, Rullkoetter PJ. Computational analysis of factors contributing to patellar dislocation. J Orthop Res 2016;34(3):444–53.
[41] Heegaard J, Leyvraz PF, Van Kampen A, Rakotomanana L, Rubin PJ, Blankevoort L. Influence of soft structures on patellar three-dimensional tracking. Clin Orthop Relat Res 1994(299):235–43. PMID:8119024
[42] Anglin C, Brimacombe JM, Wilson DR, et al. Intraoperative vs. weightbearing patellar kinematics in total knee arthroplasty: a cadaveric study. Clin Biomech (Bristol, Avon) 2008;23(1):60–70.
[43] Innocenti B, Pianigiani S, Labey L, Victor J, Bellemans J. Contact forces in several TKA designs during squatting: a numerical sensitivity analysis. J Biomech 2011;44(8):1573–81.
[44] Gasparutto X, Moissenet F, Lafon Y, Cheze L, Dumas R. Kinematics of the normal knee during dynamic activities: a synthesis of data from intracortical pins and biplane imaging. Appl Bionics Biomech 2017;2017:1908618.
[45] Mizu-Uchi H, Colwell CW Jr, Flores-Hernandez C, Fregly BJ, Matsuda S, D'Lima DD. Patient-specific computer model of dynamic squatting after total knee arthroplasty. J Arthroplasty 2015;30(5):870–4.
[46] Trepczynski A, Kutzner I, Kornaropoulos E, et al. Patellofemoral joint contact forces during activities with high knee flexion. J Orthop Res 2012;30(3):408–15.
[47] Sharma A, Leszko F, Komistek RD, Scuderi GR, Cates HE Jr, Liu F. In vivo patellofemoral forces in high flexion total knee arthroplasty. J Biomech 2008;41(3):642–8.
[48] Hellmich C, Kober C, Erdmann B. Micromechanics-based conversion of CT data into anisotropic elasticity tensors, applied to FE simulations of a mandible. Ann Biomed Eng 2008;36(1):108–22.
[49] Morgan EF, Keaveny TM. Dependence of yield strain of human trabecular bone on anatomic site. J Biomech 2001;34(5):569–77.
[50] Carter DR, Caler WE, Spengler DM, Frankel VH. Fatigue behavior of adult cortical bone: the influence of mean strain and strain range. Acta Orthop Scand 1981;52(5):481–90.
[51] Lammentausta E, Hakulinen MA, Jurvelin JS, Nieminen MT. Prediction of mechanical properties of trabecular bone using quantitative MRI. Phys Med Biol 2006;51(23):6187–98.
[52] Di Martino A, Franceschi F, Papalia R, et al. Increased bone mineral density in the non-resurfaced patella after total knee arthroplasty: a clinical and densitometric study. Surgeon 2012;10(1):20–4.
[53] Chalidis BE, Tsiridis E, Tragas AA, Stavrou Z, Giannoudis PV. Management of periprosthetic patellar fractures. A systematic review of literature. Injury 2007;38(6):714–24.
[54] Helmy N, Anglin C, Greidanus NV, Masri BA. To resurface or not to resurface the patella in total knee arthroplasty. Clin Orthop Relat Res 2008;466(11):2775–83.